Playing with the p-Doping Mechanism to Lower the Carbon Loading in n-Type Insertion Organic Electrodes: First Feasibility Study with Binder-Free Composite Electrodes

Alia Jouhara, Nicolas Dupre, Dominique Guyomard, Alae Eddine Lakraychi, Franck Dolhem, Philippe Poizot

Playing with the p-Doping Mechanism to Lower the Carbon Loading in n-Type Insertion Organic Electrodes: First Feasibility Study with Binder-Free Composite Electrodes

Journal of The Electrochemical Society, 2020 **167** 070540

Playing with the p-Doping Mechanism to Lower the Carbon Loading in n-Type Insertion Organic Electrodes: First Feasibility Study with Binder-Free Composite Electrodes

Alia Jouhara,[1] Nicolas Dupré,[1] Dominique Guyomard,[1,*] Alae Eddine Lakraychi,[2] Franck Dolhem,[3] and Philippe Poizot[1,z]

[1]*Université de Nantes, CNRS, Institut des Matériaux Jean Rouxel, IMN, F-44000 Nantes, France*
[2]*Institut de la Matière Condensée et des Nanosciences (IMCN), Université catholique de Louvain, 1348 Louvain-la-Neuve, Belgium*
[3]*Laboratoire de Glycochimie, des Antimicrobiens et des Agroressources (LG2A), UMR CNRS 7378, Université de Picardie Jules Verne, 80039 Amiens Cedex, France*

Organic electrode materials should offer promising alternative to traditional inorganic compounds thanks to several attractive assets such as low-cost, low environmental footprint or the versatility in terms of cell assemblies (cationic and/or anionic shuttling). However, improvements are needed to push forward organic solid electrodes. In particular, decrease the quantity of conductive carbon in the composite electrode is important because it impedes the resulting energy density values. Herein, we present an innovative approach aiming at replacing most of the carbon conductive additive by an electron-conductive anion-inserting crystallized organic material, namely dilithium 2,5-(dianilino)terephthalate (Li_2DAnT). Combined with an appropriate n-type lithiated organic electrode material, we demonstrate the beneficial effect of adding Li_2DAnT (23 wt%)/carbon (10 wt%) compared to a typical conducting carbon loading of 33 wt% for powder-based composite electrodes made without binder by simple mixing and grinding with a pestle in a mortar. In fact, Li_2DAnT provides an efficient percolating conductive network and contributes to the overall reversible capacity of the composite electrode through its own storage properties.
 [DOI: 10.1149/1945-7111/ab7c6d]

Manuscript submitted December 26, 2019; revised manuscript received February 28, 2020. Published March 19, 2020. *This paper is part of the JES Focus Issue on Challenges in Novel Electrolytes, Organic Materials, and Innovative Chemistries for Batteries in Honor of Michel Armand.*

Supplementary material for this article is available online

Commercially available rechargeable batteries, especially Li-based cells, may face some limitations in the near future due to the major use of scarce chemical elements (e.g., 3d transition metals) in their manufacture. In addition, the question about their potential environmental impact throughout their entire life cycle is posed considering the context of their expected massive and widespread development.[1,2] For example, a recent compilation of life cycle assessment (LCA) analyses performed on commercial Li-ion batteries (LIBs) has highlighted that a cumulative energy demand of 328 kWh is needed across all chemistries to produce 1 kWh of stored electrochemical energy together with the greenhouse gas (GHG) emissions of 110 gCO_2eq.[3] Moreover, such LCA data were obtained at the manufacturing outlet ("cradle-to-gate analyses") meaning they do not take into account both collection and recycling steps while other eco indicators such as human toxicity (HTP) are not considered. This situation calls for developing new and efficient battery chemistries easier to recycle for an affordable price and based on more abundant resources if we want to pursue the progress of our technology-oriented societies.

One possible alternative to inorganic materials lies in the development of redox-active organic materials for which the literature on the topic has been expanding since the last decade after years of silence.[2,4–10] Twenty years ago, M. Armand and co-workers[11] pointed out the interest of some redox-active hybrid organic materials to reach specific capacities higher than 500 mAh g^{-1} while Nishide's group demonstrated in the early 2000s high electron-transfer kinetics with nitroxide polymer electrodes.[12,13] Based on the assembly of the most abundant chemical elements on the Earth, organic chemistry provides also great opportunities for discovering innovative electrode functionalities thanks to molecular engineering together with access to two electrochemical storage mechanisms[10,14,15]: "n-type" electrode reactions that involve an ionic compensation with cation release upon oxidation and "p-type" electrodes reactions that imply an anion uptake. Furthermore, they can be used in non-aqueous as well as in aqueous media[16–18] including in the solubilized state for redox-flow battery applications, for which demonstrators are in progress.[19,20] However, for applications as solid organic electrodes, improvements are needed especially to increase the energy density of organic-based electrodes, which are often impeded by substantial carbon contents in the electrode formulation.[4–9] For comparison, the amount of conducting carbon in commercial Li-based batteries is less than 5%–10% of the total mass of the electrode and generally more than 20% with most organic electrodes reported in the literature. Although it should be recognized that organic compounds are often insulators[6] some options exist to overcome the problem of electronic conductivity such as favoring molecular backbones with extended electron delocalization or the decrease of the particle size.

For example, we have recently demonstrated that formulation optimization based on a processing solvent in which not only the binder but also the organic active material is soluble (controlled recrystallization process) gives rise to 86% retention of the reversible Li insertion in Indigo Carmine (IC) based electrodes over 50 cycles at C/10 rate with 10 wt% carbon only.[21] On the other hand, it is also known that some organic compounds can replace carbon when semiconducting properties appear thanks to overlap of π-orbitals, generally after p-doping. Replacing carbon by different conducting organics has already been tested with conventional inorganic electrode materials such as $LiFePO_4$ or Si.[22–24] Basically, intrinsically conducting polymers (CPs) such as polyaniline (Pani)[25,26] constitute the most common examples. Inspired by this property, Sjödin and co-workers[27] have fabricated the first all-organic proton batteries which require no conductive additives by combining redox-active pendant groups to π-conjugated p-doped

*Electrochemical Society Member.
[z]E-mail: philippe.poizot@cnrs-imn.fr

polymer backbone, resulting in so-called conducting redox polymers (CRPs). Another type of non-polymeric example is the nearly planar delocalized π-electrons (n-type) tetra-lithium perylene-3,4,9,10-tetracarboxylate salt ($PTCLi_4$) that can achieve good electrochemical performance as negative electrode with only 0.5 wt% carbon nanotubes (12.0 mg cm^{-2}, 1.2 mAh cm^{-2}) probably due to the long-range aromatic–aromatic interactions (π-stacking) within the crystal structure.[28] S. Lee et al.[29] have also recently demonstrated that the charge-transfer complex phenazine–7,7,8,8-tetracyanoquinodimethane (PNZ–TCNQ) can be cycled vs Li with only 2.5 wt% of carbon by due to its well-known intrinsic conducting properties but at 50% of the theoretical capacity. Lastly, we pinpointed few years ago that the p-type crystallized lithiated salt of 2,5-(dianilino) terephthalate (Li_2DAnT), which derives from the phenyl-capped aniline dimer, can cycle without carbon because the reversible anion ingress into the layered Li_2DAnT induces a huge change of the electrode conductivity like observed during the p-doping of Pani.[30,31]

Within this background and inspired by the works of both Deng et al.[32] and Huang et al.[33] on the partial replacement of conducting carbon by CPs to cycle n-type organic active materials (i.e., perylene-3,4,9,10-tetracharbonxydiimide (PTCDI)-doped polypyrrole and $Na_2C_6O_6$-doped Pani, respectively), we have tried for the first time to implement this approach with a non-polymeric conducting agent by choosing Li_2DAnT. Indeed, this crystallized lamellar compound[34] displays several assets. First, it can deliver a stable capacity of about 75 mAh g^{-1} (Fig. S1 is available online at stacks.iop.org/JES/167/070540/mmedia) by reversible one-electron reaction with concomitant anion ingress.[30] Second, it exhibits electronic conductive properties similarly to polyaniline.[31] Third, it can be considered as a sustainable chemical because the acid precursor (namely 2,5-(dianilino)terephthalic acid or "anilic acid") is now produced by Clariant International Ltd. from "bio-succinic acid" (renewable raw compound); the anilic acid being a key intermediate in the large scale synthesis of red and violet quinacridone pigments.[35]

To rapidly demonstrate the macroscopic efficiency of Li_2DAnT as electroactive and electronic conducting agent, two n-type lithiated positive organic electrode materials have been selected for the benchmark (dilithium (2,5-dilithium-oxy)-terephthalate, namely Li_4-*p*-DHT and tetralithium 2,5-dihydroxy-1,4-benzenedisulfonate, namely Li_4-*p*-DHBDS, Fig. S1) for which the corresponding composite electrodes have been prepared without any binder or optimized formulation, but rather through simple grinding of organic powders (Li_4-*p*-DHT–Li_2DAnT or Li_4-*p*-DHBDS–Li_2DAnT) with low amounts of conducting carbon. Interesting electrode performance has been obtained with the Li_4-*p*-DHT–Li_2DAnT blend due to the good compatibility of their respective electroactive potential window.

Experimental

Chemicals.—Reagents were purchased from commercial sources and used without further purification: 2,5-dihydroxyterephthalic acid H_4-*p*-DHT (Sigma Aldrich, ⩾98.0%), 2,5-(dianilino)terephthalic acid (Clariant), lithium hydride (Alfa Aesar), lithium methoxide (2.2 M in methanol) (Sigma Aldrich, ⩾98.0%). Lithium perchlorate (battery grade), *N*,*N*-dimethylformamide, methanol and diethylether solvents were anhydrous and purchased from Aldrich whereas propylene carbonate (PC, battery grade) was obtained from Novolyte. All synthetic reactions were conducted inside an argon-filled glove box (MBRAUN) containing less than 1 ppm of dioxygen and water (T = 30 °C).

Analytical techniques.—Infrared spectra were recorded on a FTIR Bruker Vertex 70. Air-free pellets were prepared in glove box by mixing the sample with spectroscopic-grade potassium bromide at 1 wt%. ^{1}H and ^{13}C liquid NMR spectra were recorded on a Bruker AVANCE III 400 MHz. Chemical shifts (δ) are given in ppm relative to tetramethylsilane (TMS). Deuterium oxide was purchased from Sigma Aldrich (purity higher than 99.5%). The thermogravimetry (TG)-Mass spectrometry (MS) coupled experiments were carried out with a STA449F3 Jupiter and QMS403C Aëolos instruments from NETZSCH under argon at a heating rate of 5 °C min^{-1} up to 800 °C. Scanning electron microscopy (SEM) investigations were performed on a JSM-7600F from JEOL. X-ray diffraction (XRD) patterns were recorded at room temperature with a Bruker D8 Advance powder diffractometer. Data were collected in the Bragg-Brentano geometry with a Cu-anode X-ray source operated at 40 kV and 40 mA.

Materials synthesis.— *Synthesis of dilithium (2,5-dilithium-oxy)-terephthalate (Li_4-p-DHT).*—The synthesis procedure was previously reported by Chen's group.[36] Into a homogeneous solution of H_4-*p*-DHT (1.0 g, 5.1 mmol, 1 eq.) in anhydrous methanol (50 ml) was dripped 10.1 ml of lithium methoxide (2.2 M in methanol, 22.4 mmol, 4.4 eq.). A yellow precipitate was formed after ≈3 min under stirring at room temperature. After reaction for 40 h, the as-prepared solid was filtered and washed (3 × 6 ml) with anhydrous methanol, and dried under vacuum at 100 °C overnight. The final compound Li_4-*p*-DHT was obtained by thermal treatment at 220 °C for 24 h in a drying glass oven (Büchi B-585 glassoven for drying) in glovebox to afford Li_4-*p*-DHT as orange powder (yield: 87%). The desolvation effectiveness was checked by thermal analysis and the absence of MeOH traces in NMR and IR spectra. IR (KBr pellet, cm^{-1}) 1570 (ν_{as} COO^-), 1467–1412 (ν C=C), 1363 (ν_s COO^-), 1232 (ν CO−Li), 880-800 (ν C−H); ^{1}H NMR (400 MHz, D_2O) δ (ppm) 7.11 (2H, s); ^{13}C NMR (100 MHz, D_2O) δ (ppm) 175.97 (C, C=O), 152.78 (C, C−O^-), 125.39 (C, C−COO^-), 118.82 (C, C −H).

Synthesis of tetralithium 2,5-dihydroxy-1,4-benzenedisulfonate (Li_4-p-DHBDS).—The chemical route to synthesize this salt has been previously reported by our group.[37] In short, the lithiation of 2,5-dihydroxy-1,4-benzenedisulfonic acid (1.311 g, 4.85 mmol, 1 eq.) is performed in anhydrous *N*,*N*-dimethylformamide (50 ml) with a stoichiometric amount of lithium hydride (154.0 mg, 19.4 mmol, 4 eq.). A white precipitate was formed under stirring at room temperature. After reaction for 48 h, the prepared solid was collected by centrifugation, washed 3 times with diethyl ether and dried in vacuum at 60 °C for 3 h. The observations of the as-obtained powder by SEM shows aggregates of particles with acicular morphology (Fig. S2a). The final Li_4-*p*-DHBDS was obtained in 82% yield after heating in drying glass oven at 300 °C overnight. The desolvation effectiveness was checked by thermal analysis and the absence of DMF traces in NMR and IR spectra. IR (KBr pellet, cm^{-1}) 1452 (ν C=C), 1440 (ν SO_3^-), 1208 (ν C−O), 850 (δ O−Li); ^{1}H NMR (400 MHz, D_2O) δ (ppm) 7.03 (2 H, s); ^{13}C NMR (100 MHz, D_2O) δ (ppm) 151.04 (C, C−O^-), 132.85 (C, C−SO_3^-), 118.35 (C, C−H).

Synthesis of dilithium 2,5-(dianilino)terephthalate (Li_2DAnT) .—The lithiation of 2,5-(dianilino)terephthalic acid was adapted from a procedure previously described by our group.[30] In practice, 2,5-(dianilino)terephthalic acid (1.689 g, 4.85 mmol, 1 eq.) were mixed with a stoichiometric amount of lithium hydride (77.0 mg, 9.7 mmol, 2 eq.) in anhydrous *N*,*N*-dimethylformamide (50 ml). A pale yellow precipitate was formed under magnetic stirring at room temperature. After reaction for 48 h, the prepared solid was collected by centrifugation, washed 3 times with diethyl ether and dried in vacuum at 60 °C for 3 h. The platelet morphology of the as-prepared particles observed by SEM imaging (Fig. S2b) combined with the strong Bragg peak observed at 6.5° on the powder XRD pattern (Fig. S3) confirm the lamellar structure of the as-obtained compound.[30] The final Li_2DAnT was obtained in 85% yield after thermal treatment in a drying glass oven at 250 °C overnight. The desolvation effectiveness was checked by thermal analysis and the absence of DMF traces in NMR and IR spectra (Fig. S4). IR (KBr pellet,

cm^{-1}) 3370 (ν N−H), 1600 (ν_{as} COO^-), 1570-1500 (ν C=C), 1440 (ν_s COO^-), 1280 (ν C−N), 550 (δ COO−Li); ^{1}H NMR (D_2O, 400 MHz) δ (ppm) 7.75 (2H, s), 7.44-7.40 (4H, m, H-*meta*), 7.26-7.24 (4H, m, H-*ortho*), 7.07-7.10 (2H, m, H-*para*); ^{13}C NMR (D_2O, 100 MHz) δ (ppm) 175.1 (C, C=O), 151.0 (C, C−NH), 136.2 (C, C −NHPh), 129.6 (CH, C-*meta*), 128.4 (C, C−COOLi), 121.5 (CH), 120.7 (CH, C-*para*), 118.6 (CH, C-*ortho*).

Electrochemical measurements.—The electrochemical testing of the composite electrode materials was performed in Swagelok®-type cells using a Li metal disc as the negative electrode and a Whatman® separator soaked with $LiClO_4$ 1 M in PC as the electrolyte ($V \approx 400\ \mu l$); the perchlorate anion giving the best electrochemical performance towards Li_2DAnT.[30] The composite powder-based electrodes based on the Li_4-*p*-DHT–Li_2DAnT or Li_4-*p*-DHBDS–Li_2DAnT mixtures were prepared in an argon-filled glovebox by grinding first (with a pestle in a mortar, batch of 30 mg) the two organic materials during 2 min. Then the conducting carbon (Ketjenblack EC-600JD, AkzoNobel) was added to the mixture and grinded again for 2 min more. The as-obtained mixtures were directly transferred into the cell (m_{total} = 6 mg, 5.3 mg cm^{-2}, Fig. S5) then cycled in galvanostatic mode using a MPG-2 multi-channel system (Bio-Logic SAS, Seyssinet-Pariset, France). Electrochemical Impedance Spectroscopy (EIS) measurements were performed as previously reported[31] by using a home-made Swagelok®-type 3-electrode cell connected to a VMP3 instrument (Bio-Logic SAS). The reference electrode consisted of a ring of Li metal surrounding the working electrode, whereas a Li metal disc was used as a negative electrode. The typical amplitude of the sinusoidal voltage signal used was 7 mV for frequency values ranging from 200 kHz to 10 mHz. Measurements have been performed after a relaxation period to ensure a sufficient stability of the potential ($dE/dt < 10$ mV h^{-1}).

Results and Discussion

On the contrary of our previous formulation optimization[21] aiming to fabricate low-carbon IC-based electrode tapes for which an original aqueous processing has been developed (including a controlled recrystallization of IC with carboxymethylcellulose sodium salt), no complex formulation of a slurry was intentionally performed in the present study. The carbon additive was simply grinded with the blend of organic materials (Li_4-*p*-DHT–Li_2DAnT or Li_4-*p*-DHBDS–Li_2DAnT) without binder. This extremely simple procedure has been known and applied for decades when using Swagelok-type cells.[38–40] It offers the advantage to rapidly probe the electrochemical performance of an electroactive material despite a non-optimized shaping of the electrode. Herein, our intention was to macroscopically demonstrate the beneficial effect of Li_2DAnT as both electrochemically active and non-polymeric conducting component when preparing composite electrodes in non-optimized and raw conditions.

The first tested system was the blend based on Li_4-*p*-DHT as the active n-type material because this compound is known to be highly reversible with good energy efficiency when cycled in the 2.2–3.4 V vs Li^+/Li potential range.[41] Note that the second electron is never observed in our experimental conditions[14,41] (Fig. S1a) on the contrary of the procedure reported by Chen's group,[36] which is based on a complex nanostructuration of this organic compound. Several ratios were tested but rapidly promising results were obtained with amounts of carbon adding as low as 10 wt% despite the extreme simplicity of the as-prepared composite electrodes. Therefore, we will discuss first on the electrochemical data obtained with the best blend that consists in Li_4-*p*-DHT (67 wt%)/Li_2DAnT (23 wt%)/carbon (10 wt%), denoted "Blend (67/23/10 wt%)." It is worth noting that the total amount of conducting carbon corresponds to 33% in mass that is the typical carbon ratio used in our former studies.[41–43]

Figure 1a shows the potential-specific capacity traces relative to the composite electrode made of the blend (3 representative cycles in black), together with the first cycle in red of a composite electrode based on Li_4-*p*-DHT/carbon (67/33 wt%) for the sake of comparison. As expected the blend shows an efficient reversible delithiation/lithiation process demonstrating again the high stability of this lithiated organic electrode material when cycled in carbonate-based liquid electrolyte. Compared to the typical electrochemical feature of the Li_4-*p*-DHT/carbon composite electrodes (red curve), a capacity gain is observed that can be ascribed to the shoulders located within the 3.2–3.4 V vs Li^+/Li potential range. In order to better analyze such respective electrochemical traces measured in galvanostatic mode, Fig. 1b show the corresponding incremental capacity curve obtained for the composite electrode made of the blend superimposed with the trace for both Li_4-*p*-DHT/carbon and Li_2DAnT/carbon composite electrodes in red and blue, respectively. Unambiguously, the capacity observed above 3.1 V vs Li^+/Li is related to the reversible perchlorate insertion in the Li_2DAnT host structure (one-electron reaction within the considered potential window) to form the corresponding radical cation (Fig. S1c). But the most striking feature is that with only 10 wt% of conducting carbon, the composite electrode made of the Li_4-*p*-DHT–Li_2DAnT blend exhibits very good capacity retention upon cycling with only 6% of capacity fading after 50 cycles while the adding of 33 wt% of conducting carbon leads to lower performances after 250 cycles (Fig. 2). The specific capacity evolution for the composite electrode based on Li_4-*p*-DHT/carbon (90/10 wt%) is also presented as control experiment for comparison purpose (Fig. 2). Although quite stable upon cycling, the as-observed specific capacity is lower of about 33% indicating that 10 wt% of carbon additive cannot provide a sufficiently efficient percolating conductive network. Note that an additional capability test was performed after the 50th cycle by successively applying cycling rates of 1 Li^+/5 h, 1 Li^+/2 h, 1 Li^+/1 h for 6 cycles. The collected data show that the composite electrode made of the blend (67/23/10 wt%) can sustain a stable capacity of 95 mAh g^{-1} at the highest applied current confirming that the material can handle slow to fast charge-discharge reactions without being damaged or degraded. In addition, Fig. 3 shows the electrochemical performances of another blend still at 10 wt% of carbon but containing a lower amount of Li_4-*p*-DHT (45 wt% only vs 67 wt %) combined with Li_2DAnT at the same ratio (denoted "Blend (45/45/10 wt%)"). As expected, the measured reversible capacity per gram of Li_4-*p*-DHT is higher due to the noticeable contribution of the electroactivity of Li_2DAnT to the total capacity (Fig. 3a). But the most important result is that good capacity retention can also be observed upon cycling despite the high (macroscopic) "dilution" of Li_4-*p*-DHT into the composite powder electrode, which contains only 10 wt% of conducting carbon. This experiment reinforces the above conclusions about the efficient percolating conductive network provided by Li_2DAnT.

To go further, EIS analyses were performed to analyze the interface resistance at different state of charge/discharge during the first cycle of both the best blend (67/23/10 wt%) and the composite electrode based on Li_4-*p*-DHT/carbon (90/10 wt%) for comparison purpose (Fig. 4). Nyquist diagrams for the two powder composite electrodes exhibit systematically well-defined semi-circles at higher frequencies, which is a typical behavior characterizing the charge transfer resistance in combination with the double layer capacitance. All the diagrams exhibit also the characteristic linear Warburg region at low frequencies corresponding to the diffusion of species inside the material following their transfer at its surface. Interestingly, the characteristic frequencies related to the respective semi-circles are very similar which can suggest the probing of the same limiting phenomenon and presumably the charge transfer resistance of Li_4-*p*-DHT. Although only a slight increase of impedance is observed in both cases upon cycling, one can observe that the resistance values are lower (by a factor 2) in the case of Li_4-*p*-DHT/carbon (90/10 wt%) mixture compared to the blend (67/23/10 wt%). Nevertheless, the corresponding galvanostatic curves

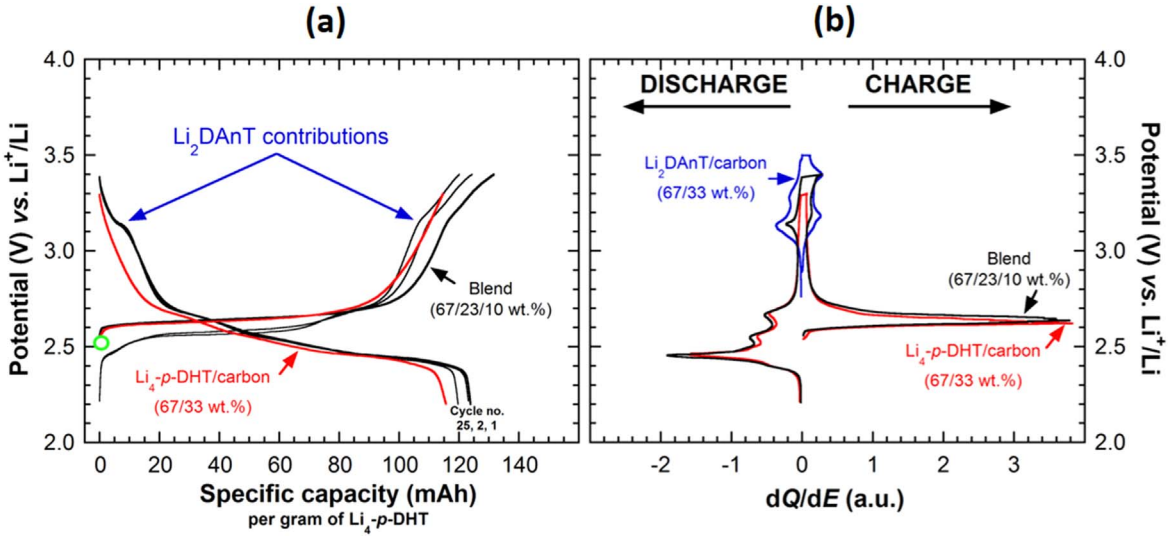

Figure 1. (a) Potential-specific capacity curves for the composite electrode based on Li_4-*p*-DHT made of the blend (67/23/10 wt%) for cycles no. 1, 2, and 25 (in black) together with the first cycle (in red) of a composite electrode based on Li_4-*p*-DHT/carbon (67/33 wt%) acquired in galvanostatic mode at a rate of 1 Li^+ exchanged per mol of Li_4-*p*-DHT in 10 h (1 Li^+/10 h, $I_m = 12.1$ mA g^{-1}). The green circle indicates the starting open circuit potential. (b) Overlay of potential vs incremental capacity d*Q*/d*E* curves (1st cycle) for the composite electrode made of the blend (in black) and Li_4-*p*-DHT/carbon 67/33 wt% (in red), respectively. For comparison, the typical trace for a composite electrode made of Li_2DAnT/carbon (67/33 wt%) is shown in blue.

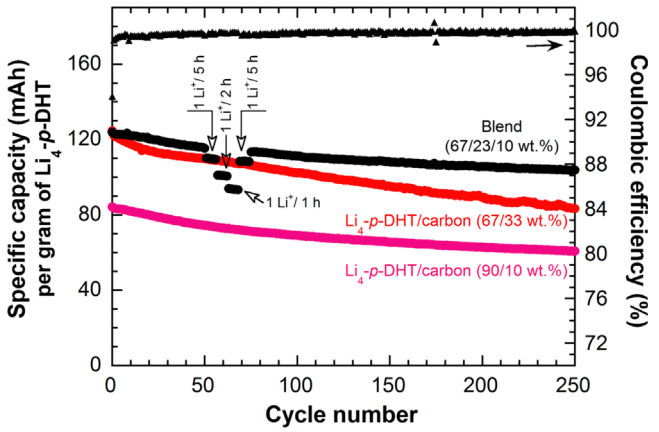

Figure 2. Capacity retention curves (in discharge) with coulombic efficiency for the composite electrode based on Li_4-*p*-DHT made of the blend (67/23/10 wt%) in black, Li_4-*p*-DHT/carbon (67/33 wt%) in red, and Li_4-*p*-DHT/carbon (90/10 wt%) in pink as control experiment. Note that a capability test was integrated after the 50th cycle by successively applying higher cycling rates for 6 cycles:1 Li^+/5 h (24.2 mA g^{-1}), 1 Li^+/2 h (60.2 mA g^{-1}), 1 Li^+/1 h (103.9 mA g^{-1}). Note that 250 cycles correspond to about 180 days in operation.

show that less than half of the practical capacity (of one exchanged electron per Li_4-*p*-DHT unit) is obtained for the (90/10 wt%) composite powder electrode (Fig. 4d) whereas the full capacity is reached with the blend (67/23/10 wt%) (Fig. 4a). Otherwise, the average polarization value corresponding to the lithium removal/uptake mechanism in Li_4-*p*-DHT appears very similar in both cases (i.e., $\Delta E \approx 160$ mV). If these low polarization values suggest an efficient percolating network in the two composite electrodes, the fact that the capacity of the electrode containing Li_4-*p*-DHT/carbon (90/10 wt%) is severely limited indicates the powder composite electrode is macroscopically not homogenous and that 10 wt% of carbon additive is not sufficient to provide electronic connection to all the active material particles. It can be estimated that only half of the particles seems connected to the percolation network giving rise to a ratio closer to 80/20 rather than the expected 90/10 in agreement with the lower measured impedance in this case. To sum up, despite the raw conditions used in the present study to prepare the composite electrodes based on Li_4-*p*-DHT, our different electrochemical measurements converge to a positive contribution of the electroactive Li_2DAnT material to the electronic percolating network.

The second system tested was based on the Li_4-*p*-DHBDS–Li_2DAnT couple. Compared to Li_4-*p*-DHT, the disulfonate counterpart is known to react at higher average potentials (i.e., $<E> \approx 3.2$ V vs Li^+/Li against 2.55 V for Li_4-*p*-DHT) according to the expected two-electron reaction (Fig. S1b). The appropriate potential range for its cycling is between 2.5 and 4.0 V vs Li^+/Li as previously reported.[37] The Li_4-*p*-DHBDS active material displays however lower electrochemical performance than Li_4-*p*-DHT upon cycling such as a noticeable charge/discharge potential difference (polarization of about 300 mV) and an irreversible capacity of 20% after the first cycle. Several ratios were also tested but larger amounts of Li_2DAnT was then considered to be added with Li_4-*p*-DHBDS because this material appears less conductive than Li_4-*p*-DHT.[37] In practice, the following ratio was selected: Li_4-*p*-DHBDS (42 wt%)/Li_2DAnT (48 wt%)/carbon (10 wt %), denoted "Blend (42/48/10 wt%)." Figure 5a shows the potential-capacity profile of the Li_2DAnT−Li_4-DHBDS blend galvanostatically cycled vs Li at a rate of 1 Li^+/10 h together with the typical first cycle of the Li_4-DHBDS/carbon composite electrode for the sake of comparison. In addition, Fig. 5b shows the corresponding incremental capacity curves for their respective first cycle to better grasp the electrochemical steps occurring in the two composite electrodes. The first charge is roughly characterized by a progressive potential increase before to reach a first plateau located at 3.3 V vs Li^+/Li followed by another one at 3.4 V as previously observed with Li_4-*p*-DHBDS/carbon (67/33 wt%) composite electrode (Fig. 5a, red trace). Then, a last plateau appears at 3.6 V corresponding to the second anion insertion into Li_2DAnT.[30] Note that this electrochemical step was not visible in Figs. 1a,b because the reverse anodic potential was limited to 3.4 V. Finally, the measured capacity after the complete charge is about 250 mAh per gram of Li_4-*p*-DHBDS, exceeding its theoretical capacity due to the 2-electron reaction involved in Li_2DAnT. With this second example, it is demonstrated again that only 10 wt% of conducting carbon allow access to the full capacity of the electroactive Li_4-*p*-DHBDS material. The electrochemical feature of the subsequent discharge curve is first characterized by the reversible reactivity of Li_2DAnT with an obvious plateau at 3.5 V corresponding to the extraction of the second anion from the host structure. Then the discharge curve shows quite

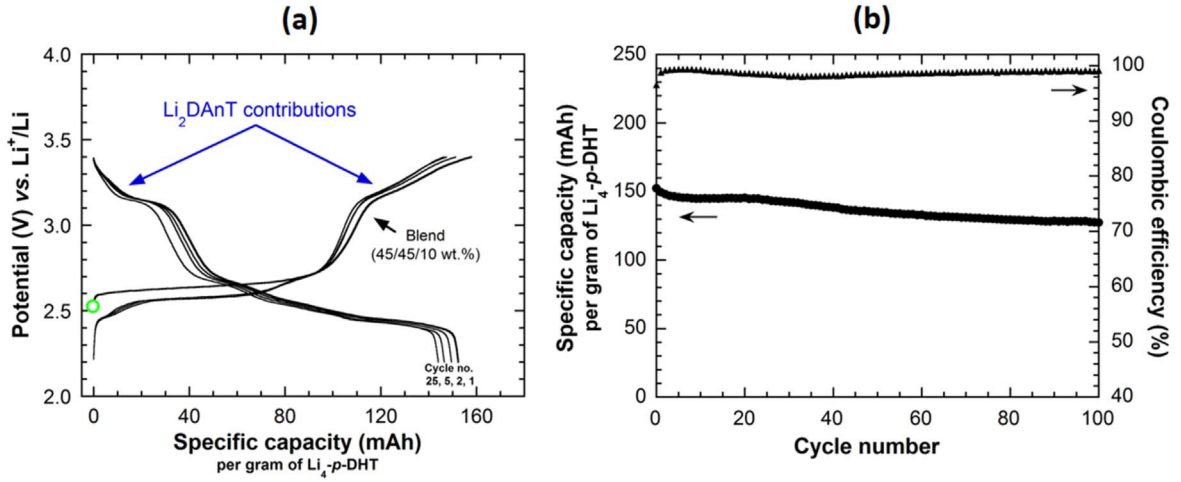

Figure 3. (a) Potential-specific capacity curves for the composite electrode based on Li_4-*p*-DHT made of the blend (45/45/10 wt%) for cycles no. 1, 2, 5, and 25 (in black). (b) Corresponding capacity retention curves (in discharge) together with coulombic efficiency.

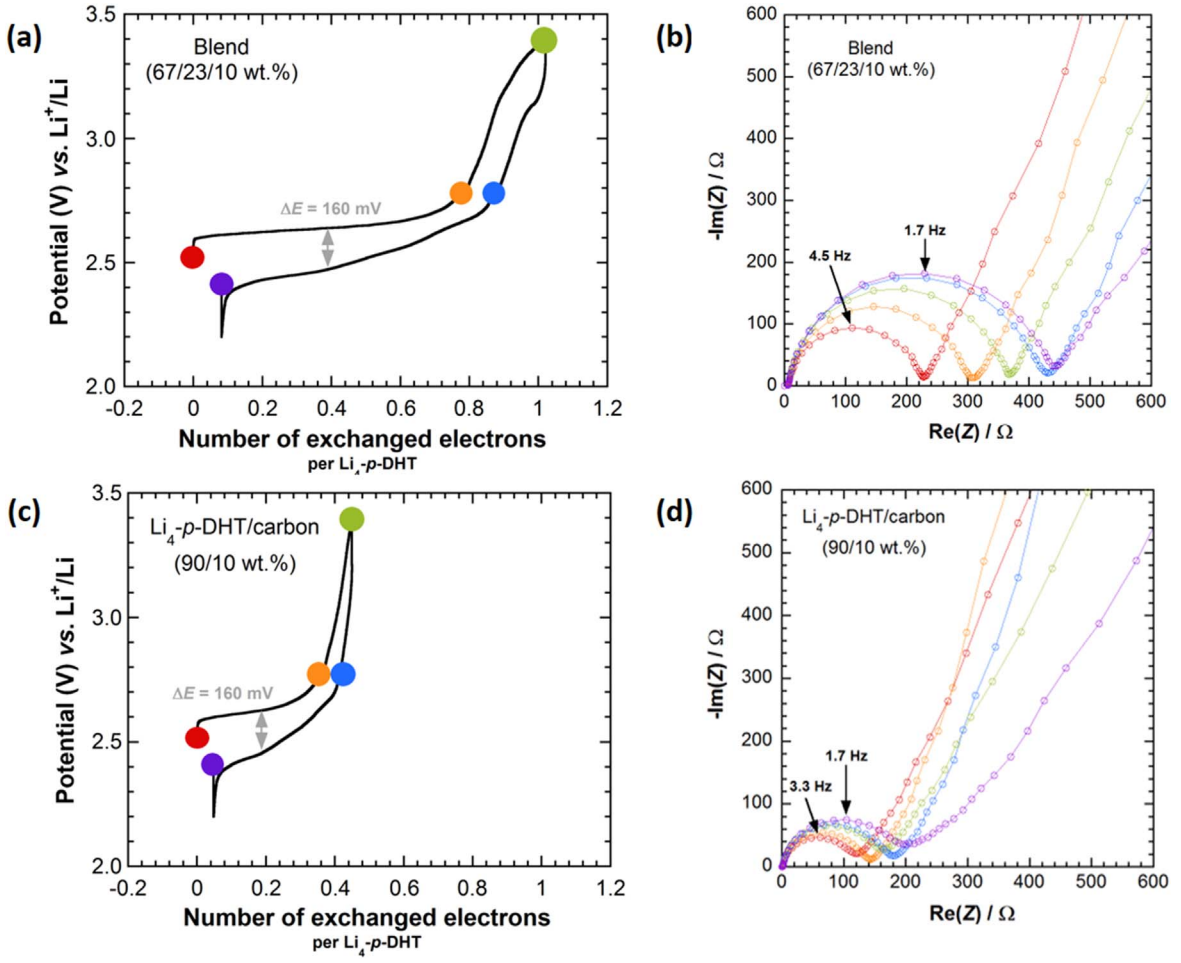

Figure 4. First galvanostatic charge/discharge curve measured in a home-made Swagelok®-type 3-electrode cell and corresponding points (with color) where EIS measurements were performed for (a) the best blend (67/23/10 wt%) based on Li_4-*p*-DHT and the composite electrode based on Li_4-*p*-DHT/carbon (90/10 wt %), respectively (reference and counter electrodes: Li; electrolyte: $LiClO_4$ 1 M in PC). (b), (d) Corresponding Nyquist diagrams.

different electrochemical behaviors compared to the expected trace for Li_4-*p*-DHBDS (Fig. 5a, red trace). In short, a series of successive electrochemical steps is observed instead of the occurrence a unique potential plateau at about 3 V (more visible in Fig. 5b) giving rise to a recovered capacity of only 190 mAh g^{-1} (irreversibility: 24%). Unfortunately, the subsequent cycles show poor stability with large capacity loss. This capacity fading is attributed here to the exfoliation phenomenon of the zwitterionic form of Li_2DAnT obtained at 3.6 V vs Li^+/Li after the insertion of two anions per DAnT moiety (Fig. S1c) and the subsequent loss of electronic conductivity initially provided by Li_2DAnT.[30,31] This assumption is well supported by the disappearance of the high-potential plateau related to the second

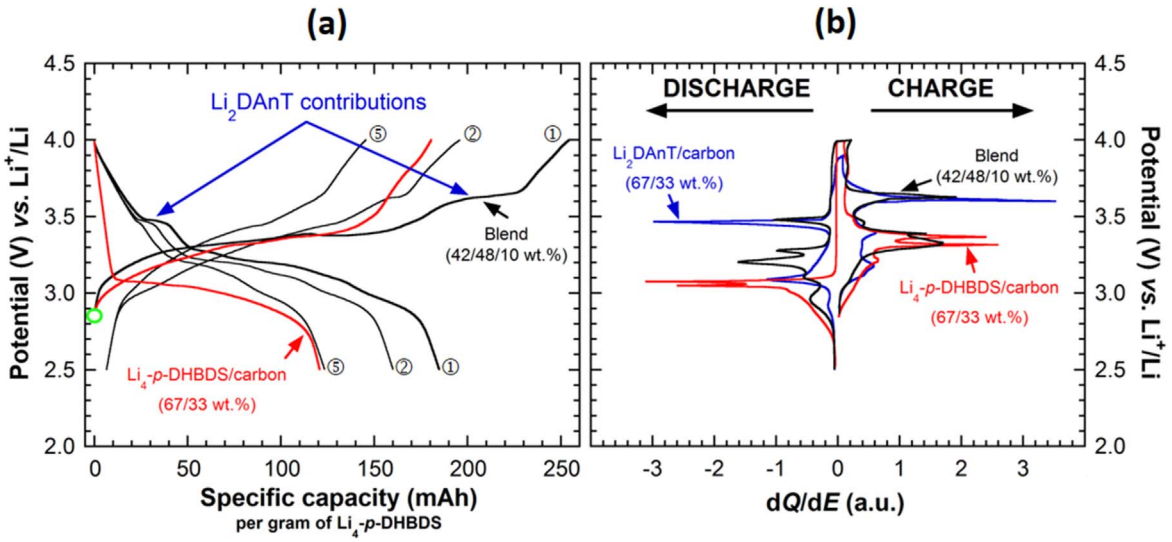

Figure 5. (a) Potential-specific capacity curves for the composite electrode based on Li_4-*p*-DHBDS made of the blend 42/48/10 wt%' for cycles no. 1, 2, and 5 (in black) together with the first cycle (in red) of a composite electrode based on Li_4-*p*-DHBDS/carbon (67/33 wt%) acquired in galvanostatic mode at a rate of 1 Li^+ exchanged per mol of Li_4-*p*-DHBDS in 10 h (1 Li^+/10 h). The green circle indicates the starting open circuit potential. (b) Overlay of potential vs incremental capacity d*Q*/d*E* curves (1st cycle) for the composite electrode based on Li_4-*p*-DHBDS made of the blend (42/48/10 wt%) in black, Li_4-*p*-DHBDS/carbon (67/33 wt%) in red, and Li_2DAnT/carbon (67/33 wt%) in blue.

insertion process occurring in Li_2DAnT. Another cell was cycled within the 2.8–3.5 V potential range to restrict the exfoliation process. A better stability upon cycling was then observed however the compatibility between the two electroactive materials Li_4-*p*-DHBDS/Li_2DAnT remains limited.

To sum up, the strong contrast in terms of electrochemical performance when comparing Li_4-*p*-DHBDS and Li_4-*p*-DHT in presence of Li_2DAnT shows that this p-type redox-active lamellar structure could be useful as both electroactive and electronic percolating additive but at the condition to applied a cut-off potential below 3.5 V vs Li^+/Li in order to suppress the poorly reversible second anion insertion. Therefore, one can anticipate that the coupling of Li_2DAnT with other n-type material working within a suitable potential window such as Li_4-*o*-DHT (2.85 V vs Li^+/Li)[43] should provide good electrochemical performances too.

Conclusions

Inspired by recent publications showing that the addition of p-type conductive polymers to n-type organic electrode materials could potentially replace the large carbon addition, we have investigated the properties of the p-type (non-polymeric) Li_2DAnT material as a "smart" and sustainable additive. Having previously established that this compound was able to reversibly intercalate anions and become electronic conductive,[30,31] composite electrodes based on either Li_4-*p*-DHT–Li_2DAnT or Li_4-*p*-DHBDS–Li_2DAnT mixtures grinded with 10 wt% carbon only were electrochemically assessed in Li half-cell. Despite the raw conditions used in the present study to prepare the composite electrodes (simple powder grinding without binder), we demonstrate in the case of Li_4-*p*-DHT that the 2-D Li_2DAnT structure could efficiently replace the carbon additive limiting therefore the dead mass of the composite electrode thanks to its faradaic contribution to the reversible capacity by anion insertion/deinsertion. Nevertheless, poor electrochemical performances were obtained when using the Li_4-*p*-DHBDS–Li_2DAnT blend notably due to the overall 2-electron reaction occurring in Li_2DAnT that induces exfoliation of its lamellar structure and subsequent degradation of the composite electrode. Hence the excellent electrochemical performance of Li_4-*p*-DHT–Li_2DAnT blend is attributed to the stability and conductivity of Li_2DAnT in the 2.2–3.4 V vs Li^+/Li potential range. Mixing Li_2DAnT with other compatible redox active materials should behave similarly.

Acknowledgments

This work funded by the University of Nantes. The authors wish specially to thank M. Armand from CIC Energigune (Spain) for the collaborative works in organic batteries, the laboratory CEISAM (UMR CNRS 6230) in Nantes for complementary experiments as well as S. Ohren (Clariant International Ltd., Switzerland) for providing 2,5-(dianilino)terephthalic acid ("anilic acid") and support to this research.

ORCID

Philippe Poizot https://orcid.org/0000-0003-1865-4902

References

1. P. Poizot and F. Dolhem, *Energy Environ. Sci.*, **4**, 2003 (2011).
2. P. Poizot, J. Gaubicher, S. Renault, L. Dubois, Y. Liang, and Y. Yao, *Chem. Rev.*, In Press.
3. J. F. Peters, M. Baumann, B. Zimmermann, J. Braun, and M. Weil, *Renew. Sustain. Energy Rev.*, **67**, 491 (2017).
4. Y. Liang, Z. Tao, and J. Chen, *Adv. Energy Mater.*, **2**, 742 (2012).
5. Z. Song and H. Zhou, *Energy Environ. Sci.*, **6**, 2280 (2013).
6. B. Häupler, A. Wild, and U. S. Schubert, *Adv. Energy Mater.*, **5**, 1402034 (2015).
7. T. B. Schon, B. T. McAllister, P. F. Li, and D. S. Seferos, *Chem. Soc. Rev.*, **45**, 6345 (2016).
8. S. Lee, G. Kwon, K. Ku, K. Yoon, S. K. Jung, H. D. Lim, and K. Kang, *Adv. Mater.*, **30**, 1704682 (2018).
9. Y. Liang and Y. Yao, *Joule*, **2**, 1690 (2018).
10. P. Poizot, F. Dolhem, and J. Gaubicher, *Curr. Opin. Electrochem.*, **9**, 70 (2018).
11. N. Ravet, C. Michot, and M. Armand, *MRS Proc.*, **496** (1997).
12. H. Nishide, S. Iwasa, Y. J. Pu, T. Suga, K. Nakahara, and M. Satoh, *Electrochim. Acta*, **50**, 827 (2004).
13. T. Suga, Y. J. Pu, K. Oyaizu, and H. Nishide, *Bull. Chem. Soc. Jpn.*, **77**, 2203 (2004).
14. A. Jouhara, N. Dupré, A. C. Gaillot, D. Guyomard, F. Dolhem, and P. Poizot, *Nat. Commun.*, **9** (2018).
15. A. Jouhara, E. Quarez, F. Dolhem, M. Armand, N. Dupré, and P. Poizot, *Angew. Chem. Int. Ed.*, **58**, 15680 (2019).
16. K. Hatakeyama-Sato, H. Wakamatsu, R. Katagiri, K. Oyaizu, and H. Nishide, *Adv. Mater.*, **30**, 1800900 (2018).
17. S. Perticarari, T. Doizy, P. Soudan, C. Ewels, C. Latouche, D. Guyomard, F. Odebel, P. Poizot, and J. Gaubicher, *Adv. Energy Mater.*, **9**, 1803688 (2019).
18. S. Perticarari et al., *Chem. Mater.*, **31**, 1869 (2019).
19. X. Wei et al., *ACS Energy Lett.*, **2**, 2187 (2017).
20. W. Liu, W. Lu, H. Zhang, and X. Li, *Chem. - Eur. J.*, **25**, 1649 (2019).
21. E. Deunf, P. Poizot, and B. Lestriez, *J. Electrochem. Soc.*, **166**, A747 (2019).
22. Q. Wang, N. Evans, S. M. Zakeeruddin, I. Exnar, and M. Grätzel, *J. Am. Chem. Soc.*, **129**, 3163 (2007).
23. G. Liu, S. Xun, N. Vukmirovic, X. Song, P. Olalde-Velasco, H. Zheng, V. S. Battaglia, L. Wang, and W. Yang, *Adv. Mater.*, **23**, 4679 (2011).

24. P. Sengodu and A. D. Deshmukh, *RSC Adv.*, **5**, 42109 (2015).
25. E. M. Geniès, A. Boyle, M. Lapkowski, and C. Tsintavis, *Synth. Met.*, **36**, 139 (1990).
26. P. Novák, K. Müller, K. S. V. Santhanam, and O. Haas, *Chem. Rev.*, **97**, 207 (1997).
27. R. Emanuelsson, M. Sterby, M. Strømme, and M. Sjödin, *J. Am. Chem. Soc.*, **139**, 4828 (2017).
28. A. Iordache, D. Bresser, S. Solan, M. Retegan, M. Bardet, J. Skrzypski, L. Picard, L. Dubois, and T. Gutel, *Adv. Sustain. Syst.*, **1**, 1600032 (2017).
29. S. Lee et al., *Energy Storage Mater.*, **20**, 462 (2019).
30. E. Deunf, P. Moreau, E. Quarez, D. Guyomard, F. Dolhem, and P. Poizot, *J. Mater. Chem. A*, **4**, 6131 (2016).
31. E. Deunf, N. Dupré, E. Quarez, P. Soudan, D. Guyomard, F. Dolhem, and P. Poizot, *CrystEngComm*, **18**, 6076 (2016).
32. W. W. Deng, Y. F. Shen, X. M. Liang, J. W. Feng, and H. X. Yang, *Electrochim. Acta*, **147**, 426 (2014).
33. Y. Huang, G. Jiang, J. Xiong, C. Yang, Q. Ai, H. Wu, and S. Yuan, *Appl. Surf. Sci.*, **499**, 143849 (2020).
34. E. Quarez, E. Deunf, V. Cadiou, T. Gutel, F. Boucher, D. Guyomard, and P. Poizot, *CrystEngComm*, **19**, 6787 (2017).
35. High Performance Pigments, Clariant webpage, https://clariant.com/en/Business-Units/Pigments/Coatings/Quinacridone last accessed December 2019.
36. S. Wang, L. Wang, K. Zhang, Z. Zhu, Z. Tao, and J. Chen, *Nano Lett.*, **13**, 4404 (2013).
37. A. E. Lakraychi, E. Deunf, K. Fahsi, P. Jimenez, J. P. Bonnet, F. Djedaini-Pilard, M. Bécuwe, P. Poizot, and F. Dolhem, *J. Mater. Chem. A*, **6**, 19182 (2018).
38. E. Wang, J. M. Tarascon, and S. Colson, *J. Electrochem. Soc.*, **138**, 166 (1991).
39. J. M. Tarascon and D. Guyomard, *J. Electrochem. Soc.*, **138**, 2864 (1991).
40. P. Poizot, S. Laruelle, S. Grugeon, L. Dupont, and J.-M. Tarascon, *Nature*, **407**, 496 (2000).
41. S. Renault, S. Gottis, A. L. Barrès, M. Courty, O. Chauvet, F. Dohlem, and P. Poizot, *Energy Environ. Sci.*, **6**, 2124 (2013).
42. S. Renault, J. Geng, F. Dolhem, and P. Poizot, *Chem. Commun.*, **47**, 2414 (2011).
43. S. Gottis, A. L. Barrès, F. Dolhem, and P. Poizot, *ACS Appl. Mater. Interfaces*, **6**, 10870 (2014).